Electrochemistry and Infrared Spectroelectrochemistry of the Substituted Phosphine Complexes, $XTa(CO)_4(dppe)$ (X = I, Br) and $XM(CO)_2(dppe)_2$ (X = H, I, Br ,Cl; M= Nb, Ta)

Christine A. Blaine, John E. Ellis, and Kent R. Mann*

Department of Chemistry, University of Minnesota, Minneapolis, Minnesota 55455

Received September 7, 1994[⊗]

The electrochemistry and spectroelectrochemistry of the substituted group V carbonyl complexes $XTa(CO)_4(dppe)$ (X = I, Br) and $XM(CO)_2(dppe)_2$ (X = I, Br, Cl, H; dppe = 1,2 bis(diphenylphosphino)ethane; M = Nb, Ta) have been investigated. The $XTa(CO)_4(dppe)$ tetracarbonyl species exhibit irreversible oxidations at E_a = +868 mV (X^- = Br^-) and E_a = +1276 (X^- = I^-) mV. Spectroelectrochemical oxidation of these complexes at E_{app} = +1000 mV indicates that CO is evolved with decomposition to non-carbonyl containing products. The reduction chemistry of $ITa(CO)_4(dppe)$ showed an irreversible cathodic process at E_c = −1541 mV in $TBA^+PF_6^-$/THF with two coupled oxidation processes (at E_a = −530 mV and E_a = +100 mV). Spectroelectrochemical reduction of $ITa(CO)_4(dppe)$ generates $Ta(CO)_4(dppe)^-$; oxidation of the anion produces $ITa(CO)_4(dppe)$ at the first coupled process and $HTa(CO)_4(dppe)$ at the second, respectively. The more highly substituted $XM(CO)_2(dppe)_2$ compounds each exhibit a one-electron reversible oxidative process in $CH_2Cl_2/TBA^+PF_6^-$ ($E°$ ca. −270 to +110 mV) that generate stable (electrochemical time scale) 17-electron species, ($XM(CO)_2(dppe)_2^+$) that were also characterized by IR spectroelectrochemical techniques. EPR spectra observed for these radical cations exhibit ten line signals at g = 2.04 (X^- = Cl^-) and g = 2.05 (X^- = H^-) with characteristic coupling to ^{93}Nb (I = $^9/_2$) (A = 115 G for X^- = Cl^-; A = 113 G for X^- = H^-). Attempts to isolate salts of the $XM(CO)_2(dppe)_2^+$ species were unsuccessful.

Introduction

The reductive coupling reactions of the carbonyl ligands in low valent, phosphine-substituted niobium and tantalum carbonyl compounds has been an important area of research.[1] Until very recently,[2] potential intermediates in these reactions (i.e. zerovalent tantalum and niobium carbonyl complexes[3]) have been detected only with matrix isolation techniques.[4] Although electrochemical and spectroelectrochemical methods are useful for observing transient species,[5] few electrochemical studies of substituted carbonyl complexes of group V have been performed. A previous electrochemical study of group VI phosphine substituted carbonyls[6] led Wreford *et al.*,[7] to investigate the oxidation of $XM(CO)_2(LL)_2$, (M = Nb, Ta; X = Cl, Br, I; LL = dmpe). Each species exhibited a one-electron reversible oxidation process that produced a putative 17-electron species as the product. The oxidation products were stable on the electrochemical time scale; however, attempts to isolate and/or characterize the reactive radical species were unsuccessful.

In this paper, we describe electrochemical and spectroelectrochemical investigations of $XM(CO)_4(dppe)$, (X = Br, I; M = Ta;) and $XM(CO)_2(dppe)_2$, (X = I, Br, Cl, H; M = Nb, Ta). The variation of phosphine, metal and halide on the stability of these complexes has been investigated. The flow-through, thin layer bulk electrolysis cell previously described[8] has enabled us to characterize 17-electron radical species ($ClNb(CO)_2(dppe)_2^+$ and $HNb(CO)_2(dppe)_2^+$) by EPR spectroscopy. Improved syntheses of $HNb(CO)_2(dppe)_2$ and $HTa(CO)_2(dppe)_2$ are also described.

Experimental Procedure

General Procedures and Starting Materials. Operations were performed under an atmosphere of argon purified by passage through columns of activated BASF catalyst and molecular sieves. All manipulations were done on a double-manifold vacuum line. Solid starting materials and synthesized compounds were handled and stored in a Vacuum Atmosphere Corp. glovebox under purified argon and nitrogen. Solutions were transferred via stainless steel cannula or glass syringes equipped with nylon stopcocks and stainless steel needles. Tetrahydrofuran (THF), 1,2-dimethoxyethane (DME), and diethyl ether (Et_2O) were distilled at atmospheric pressure from solutions of benzophenone radical, with diglyme added in the cases of ether to help solubilize the alkali metal cation. Toluene and *n*-heptane were distilled from sodium metal. Dichloromethane and acetonitrile were degassed by bubbling with nitrogen and then distilled from CaH_2 under argon prior to use. Silver hexafluorophosphate and triphenylcarbenium hexafluorophosphate were obtained from Aldrich and used without further purification. The 40% Na(Hg)[9] and ferrocenium hexafluorophosphate[10] were prepared as reported in the literature. $ITa(CO)_4(dppe)$ and $BrTa(CO)_4(dppe)$ were synthesized as reported by Calderazzo *et al.*[3f] $ITa(CO)_2(dppe)_2$, $INb(CO)_2(dppe)_2$, $BrNb(CO)_2(dppe)_2$, and $ClNb(CO)_2(dppe)_2$ were synthesized by a similar method, but 2 equiv of dppe

* To whom correspondence should be addressed.
[⊗] Abstract published in *Advance ACS Abstracts,* February 15, 1995.

(1) (a) Bianconi, P. A.; Vrtis, R. N.; Rao, Ch. P.; Williams, I. D.; Engeler, M. P.; Lippard, S. J. *Organometallics* **1987**, *6*, 1968. (b) Vrtis, R. N.; Lui, S.; Rao, Ch. P.; Bott, S. G.; Lippard, S. J. *Organometallics* **1991**, *10*, 275.
(2) Koeslag, M. D.; Baird, M. C. *Organometallics* **1994**, *13* , 11.
(3) (a) Calderazzo, F.; Pampaloni, G. *J. Organomet. Chem.* **1992**, *423*, 307. (b) Calderazzo, F.; Pampaloni, G.; Zanazzi, P. F. *J. Chem. Soc., Chem. Commun.* **1982**, 1304. (c) Calderazzo, F.; Pampaloni, G. *J. Organomet. Chem.* **1986**, *303*, 111. (d) Calderazzo, F.; Castellani, M.; Pampaloni, G.; Zanazzi, P. F. *J. Chem. Soc., Dalton Trans.* **1985**, 1989. (e) Calderazzo, F.; Pampaloni, G.; Pelizzi, G.; Vitali, F. *Organometallics* **1988**, *7*, 1083.
(4) DeKock, R. L. *Inorg. Chem.* **1971**, *10*, 1025.
(5) Hill, M. G.; Sykes, A. G. Mann, K. R. *Inorg. Chem.* **1993,** *32*, 783.
(6) Pickett, C. J.; Pletcher, D. J. *J. Organomet. Chem.* **1975**, *102*, 327.
(7) Bond, A. M.; Bixler, J. W.; Morcellini, E.; Datta, S.; James, E. J.; Wreford, S. S. *Inorg. Chem.* **1980**, *19*, 1760.
(8) Hill, M. G. Ph.D. Dissertation. University of Minnesota, 1992.
(9) Babcock, S. H. *Inorg. Synth.* **1939**, *1*, 10.
(10) Duggan, M. D.; Gray, H. B. *Inorg. Chem.* **1975**, *14*, 955.

0020-1669/95/1334-1552$09.00/0

were added. The resulting compounds gave physical data comparable to those reported in the literature.[11]

Infrared spectra were recorded with a Mattson 6021 Galaxy spectrometer using sealed 0.1 mm path length NaCl and CaF_2 cells fitted with nylon stopcocks. NMR spectra (samples in sealed 5 mm tubes) were recorded with Bruker 200-T and Varian Unity 300 spectrometers. EPR spectra (samples sealed in 5 mm tubes) were recorded with an IBM-Bruker ESP-300 spectrometer, equipped with a specially designed low temperature EPR dewar. The magnetic field was calibrated with 2,2-diphenyl-1-picrylhydrazyl hydrate, DPPH (g = 2.0037).[12] Microanalyses were carried out by Analytische Laboratorien, Engelskirchen, Germany.

$HNb(CO)_2(dppe)_2$. The following procedure is an improvement over the previous method reported by Rehder *et al.*[13,14] An orange solution resulted upon addition of 10 mL of THF to $INb(CO)_2(dppe)_2$, (1.059 g, 1.11 mmol). Excess 40% Na(Hg) (2 mL) was added via syringe to the THF solution. A dark red solution resulted above the stirring sodium amalgam. The solution was allowed to stir for 5 h. The solution was filtered through diatomaceous earth to remove excess sodium amalgam. A blood red solution remained. Excess EtOH, (10 mL), was added to the solution and allowed to stir at room temperature overnight. A precipitate was present after 12 h. The THF volume was reduced to 5 mL and 25 mL of n-heptane was added. The red-orange precipitate was filtered by inversion and dried in vacuo for 2 h. The solid was recrystallized from toluene/Et_2O. A reddish-orange solid was isolated in 85% yield. IR (THF): ν(CO) 1775 cm^{-1}. IR (mull): ν(CO) 1768 cm^{-1}. ^1H NMR (200 MHz, benzene-d_6, 23 °C): −4.10 ppm (tt; J(P−H): 98, 18 Hz). ^{31}P NMR (200 MHz, benzene-d_6, 23 °C): 80.4 ppm (s), 58.0 ppm (s). Anal. Calcd for $NbO_2P_4C_{54}H_{49}$: C, 68.51; H, 5.22. Found: C, 68.45, H, 5.50.

$HTa(CO)_2(dppe)_2$. A procedure similar to that used for the niobium analog was used. Excess 40% Na(Hg), (1.544 g, 1.33 mmol) of $ITa(CO)_2(dppe)_2$, and EtOH were used. The solid was recrystallized from toluene/Et_2O. An orange-red solid was isolated in 55% yield. IR (THF): ν(CO) 1764 cm^{-1}. IR (mull): ν(CO) 1753 cm^{-1}. ^1H NMR (200 MHz, benzene-d_6, 23 °C): −3.19 ppm (tt; J(P−H): 100, 22 Hz). ^{31}P NMR (200 MHz, benzene-d_6, 23 °C): 47.9 ppm (s), 68.2 ppm (s). Anal. Calcd for $TaO_2P_4C_{54}H_{49}$: C, 62.68; H, 4.77. Found: C, 62.44; H, 4.99.

Electrochemical Measurements. All electrochemical experiments were performed with a BAS 100 electrochemical analyzer unless otherwise noted. Cyclic voltammetry (CV) and chronocoulometry (CC) experiments were performed at ambient temperature (23 °C) with a normal three-electrode configuration consisting of a highly polished glassy-carbon-disk working electrode (A = 0.07 cm^2), and a Ag/AgCl reference electrode containing 1.0 M KCl. The working compartment of the electrochemical cell was separated from the reference compartment by a modified Luggin capillary. All three compartments contained a 0.1 M solution of supporting electrolyte. Tetrabutylammonium hexafluorophosphate ($TBA^+PF_6^-$) was used without further purification. Tetrabutylammonium tetrafluoroborate was dried in a drying pistol overnight at 110 °C. ($TBA^+BF_4^-$). All of the supporting electrolytes were purchased from Southwestern Analytical Chemicals, Inc. In most cases, the electrolyte and solvent were passed down an alumina column prior to the electrochemical experiments. In all cases, working solutions were prepared by recording background cyclic voltammograms of the electrolyte solution before addition of the complex. The working compartment of the cell was bubbled with solvent-saturated argon to deaerate the solution.

Potentials are reported versus aqueous Ag/AgCl and are not corrected for the junction potential. A standard electrochemical current convention is used (anodic currents are negative). To allow future corrections and the correlation of these data with other workers, we have measured the $E^{\circ\prime}$ for the ferrocenium/ferrocene couple under conditions identical to those used for the compounds under study. In the 25 mL electrochemical cell, values were 0.1 M $TBA^+PF_6^-/CH_2Cl_2$, $E^{\circ\prime}$ = +0.46 V; in 0.1 M $TBA^+PF_6^-/CH_3CN$, $E^{\circ\prime}$ = +0.51 V; in 0.1 M $TBA^+PF_6^-$/THF versus Pt pseudo reference electrode $E^{\circ\prime}$ = +0.64 V. In the 10 mL electrochemical cell used for the $ITa(CO)_4(dppe)$ experiments, the ferrocenium/ferrocene couple occurred at $E^{\circ\prime}$ = +0.45 V in 0.1 M $TBA^+PF_6^-/CH_2Cl_2$. No iR compensation was used. Bulk electrolyses were performed with a platinum mesh electrode.

EPR samples were produced by oxidizing a solution with a thin-layer, flow through bulk electrolysis cell.[8]

Spectroelectrochemical Experiments. Infrared spectral changes accompanying thin-layer bulk electrolysis were measured using a flow-through thin-layer spectroelectrochemical cell.[8] All spectroelectrochemical experiments were performed with a Mattson 6021 Galaxy spectrometer and a BAS 100 instrument.

Results

Electrochemical Studies of $XTa(CO)_4(dppe)$, (X = Br, I) in 0.1 M $TBA^+PF_6^-/CH_3CN$, 0.1 M $TBA^+PF_6^-/CH_2Cl_2$ and 0.1 M $TBA^+PF_6^-$/THF. Initial attempts to study the electrochemistry of $BrTa(CO)_4(dppe)$ in acetonitrile solutions suggested that $BrTa(CO)_4(dppe)$ decomposed over the course of 30 min at room temperature in this solvent; however, solutions in CH_2Cl_2 and THF were stable. $BrTa(CO)_4(dppe)$ exhibits two anodic electrochemical processes in 0.1 M $TBA^+PF_6^-/CH_2Cl_2$: an irreversible multielectron process at E_a = +868 mV and another irreversible process at E_a = +1276 mV. Reduction of $BrTa(CO)_4(dppe)$ occurs in an irreversible process at E_c = −1332 mV with coupled anodic processes at E_a = −742 mV and E_a = ~121 mV. Chronocoulometry experiments (E_i = 0 to E_f = −1800 mV) gave a diffusion coefficient of 4.05 × 10^{-6} cm^2/sec for n = 2 electrons.

The electrochemistry of the iodo analog was also studied in 0.1 M $TBA^+PF_6^-/CH_2Cl_2$ and 0.10 M $TBA^+PF_6^-$/THF. As in the Br^- case, in 0.1 M $TBA^+PF_6^-/CH_2Cl_2$, two irreversible processes at E_a = +850 mV and E_a = +1234 mV resulted upon oxidation of $ITa(CO)_4(dppe)$.

Oxidation of $ITa(CO)_4(dppe)$ in the infrared spectroelectrochemical cell at potentials positive of the first anodic process at E_{app} = +1000 mV cause the starting material carbonyl peaks at 2023, 1946, 1905, and 1884 cm^{-1} to disappear, but no new carbonyl containing products result. CO evolution was evident from the growth of a small band at 2138 cm^{-1}. The second oxidation process at E_a = +1302 mV was not studied.

Reduction of $ITa(CO)_4(dppe)$ in 0.1 M $TBA^+PF_6^-/CH_2Cl_2$, occurs in a single cathodic process with two coupled anodic processes. The cathodic process is irreversible (E_c = −1731 mV), and very near the solvent limit of CH_2Cl_2; the two coupled return peaks are observed at E_a = −708 mV and E_a = −21 mV. When the cyclic voltammogram was initiated at E_i = −1000 mV in the postive direction with limits of +300 and −1800 mV, both of the waves at −708 and −21 mV disappeared. An increase in the scan rate to 500 mV/s did not improve the reversibility of this process.

Better electrochemical data for the reduction wave of $ITa(CO)_4(dppe)$ were obtained from solutions 0.10 M $TBA^+PF_6^-$/THF, a solvent/electrolyte combination with a larger window of +2.0 to −3.0 V.[15] A cyclic voltammogram of the reduction of $ITa(CO)_4(dppe)$ in 0.10 M $TBA^+PF_6^-$/THF is shown in Figure 1. A single irreversible cathodic process was observed at E_c = −1541 mV with coupled return processes at E_a = −530 mV and E_a = +100 mV. Chronocoulometry experiments are consistent with n = 2 (D = 2.19 × 10^{-6} cm^2/s) for the large irreversible wave at −1541 mV. Chronocoulometry results for

(11) Brown, L. D.; Datta, S.; Kouba, J. K.; Smith, L. K.; Wreford, S. S. *Inorg. Chem.* **1974**, *16*, 1134.
(12) Drago, S. *Physical Methods in Chemistry*; W. B. Saunders Co.: Philadelphia, PA, 1977.
(13) Bechthold, H.; Rehder, D. *J. Organomet. Chem.* **1982**, *223*, 215.
(14) Fornalczyk, M.; Oltmanns, P.; Rehder, D. *J. Organomet. Chem.* **1987**, *331*, 207.
(15) Supporting electrolyte = $TBA^+PF_6^-$; Pt wire reference electrode; $E^{\circ\prime}$ for ferrocene/ferrocenium in 0.10 M $TBA^+PF_6^-$/THF versus Pt electrode was 0.64 V.

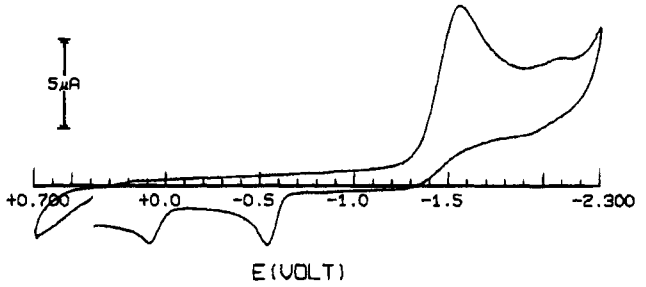

Figure 1. Cyclic voltammogram of $ITa(CO)_4(dppe)$ in 0.1 M $TBA^+PF_6^-$/THF with a Pt wire as the reference electrode. $E^{\circ\prime} = 0.64$ V for ferrocenium/ferrocene couple versus Pt electrode in THF at a scan rate of 100 mV/s.

the wave at $E_a = -530$ mV showed the number of electrons passed to be approximately one-third of the value of the two-electron reduction wave at $E_c = -1541$ mV. The process at $E_a = +100$ mV showed the number of electrons passed to be ca. one-half of the two-electron reduction process.

Reduction of $ITa(CO)_4(dppe)$ in the infrared spectroelectrochemical cell at $E_{app} = -2000$ mV is shown in Figure 2.[16] The starting material peaks at 2020, 1944, 1904, and 1884 cm^{-1} are replaced on reduction by peaks due to $Ta(CO)_4(dppe)^-$ at 1906, 1800, 1778, and 1753 cm^{-1} and a broad peak (1867 cm^{-1}) and a smaller peak (1998 cm^{-1}) assigned to $HTa(CO)_4(dppe)$. $HTa(CO)_4(dppe)$ forms from trace amounts of water reacting with the anion. This reaction explains the nonisosbestic character of the electrochemical reduction. Upon further reduction at $E_{app} = -2000$ mV, the small amount of hydride generated was reduced to the anion.

Oxidation of electrogenerated anion at the first coupled anodic process ($E_{app} = -300$ mV) regenerates $ITa(CO)_4(dppe)$ and produces $HTa(CO)_4(dppe)$ as shown in Figure 3. Oxidations more positive than the second coupled anodic process result in conversion of the hydride (IR peaks at 1867 and 1998 cm^{-1}) to the starting material $ITa(CO)_4(dppe)$ (peaks at 2020, 1994, 1904, and 1884 cm^{-1}). Similar results occur for the reduction of $ITa(CO)_4(dppe)$ in 0.1 M $TBA^+PF_6^-/CH_2Cl_2$ at $E_{app} = -2000$ mV.

The assignment of the observed carbonyl stretching frequencies at 1867 and 1998 cm^{-1} to $HTa(CO)_4(dppe)$, were confirmed by repeating the experiment in the presence of added water. The reduction of the starting material at $E_{app} = -2000$ mV in this case gave infrared spectra that showed more of the hydride compound. Oxidation of the anion generated by reduction of $ITa(CO)_4(dppe)$ at $E_{app} = -300$ mV gave only carbonyl peaks corresponding to the hydride.[17] Further oxidation at $E_{app} = +300$ mV resulted in the isosbestic conversion of $HTa(CO)_4(dppe)$ to $ITa(CO)_4(dppe)$.

Electrochemical Studies of $XM(CO)_2(dppe)_2$ in 0.1 M $TBA^+PF_6^-/CH_2Cl_2$, Where X = I, Br, and Cl and M = Nb and Ta. The cyclic voltammogram of $ClNb(CO)_2(dppe)_2$ in 0.1 M $TBA^+PF_6^-/CH_2Cl_2$ is shown in Figure 4. Oxidation results in two redox processes: a one-electron reversible process at $E^{\circ\prime} = -7$ mV ($i_{pc}/i_{pa} = 1.0$) versus Ag/AgCl and an irreversible multielectron process at $E_a = +960$ mV.

The first process is assigned as a reversible one-electron oxidation to a 17-electron species as shown in eq 1.

$$ClNb(CO)_2(dppe)_2 \rightleftharpoons ClNb(CO)_2(dppe)_2^+ + e^- \quad (1)$$

This 17-electron radical is stable on the electrochemical time scale and is similar to a radical species proposed for tantalum analogs reported by Wreford *et al.*[6] Similarily, bulk electrolysis of $BrNb(CO)_2(dppe)_2$ at $E_{app} = +300$ mV gives $n = 1.1 \pm 0.1$ electrons. Chronocoulometry experiments are consistent with $n = 1$ electron as shown in Table 1.

Infrared spectroelectrochemical data for the one-electron oxidation of $ClNb(CO)_2(dppe)_2$ in 0.1 M $TBA^+PF_6^-/CH_2Cl_2$ are shown in Figure 5. The electrolysis of $ClNb(CO)_2(dppe)_2$ in the infrared cell at $E_{app} = +400$ mV shows the isosbestic conversion to the stable cationic species $ClNb(CO)_2(dppe)_2^+$ with $\nu(CO)$ at 1944 and 1869 cm^{-1}. Reduction of this cationic species at $E_{app} = -300$ mV quantitatively regenerated the neutral compound. Spectroelectrochemical oxidations of the 17-electron species at $E_a = +960$ mV were not performed.

The electrochemical and the spectroelectrochemical results obtained for other $XM(CO)_2(dppe)_2$ (X = Br, I; M = Nb, Ta) compounds are similar and are shown in Tables 1 and 2. The oxidation of the niobium compounds follow the trend I > Br > Cl, with $INb(CO)_2(dppe)_2$ the most difficult to oxidize and the $ClNb(CO)_2(dppe)_2$ the easiest to oxidize; additionally, $ITa(CO)_2(dppe)_2$ was easier to oxidize than $INb(CO)_2(dppe)_2$.

The cyclic voltammograms of $ITa(CO)_2(dppe)_2$, $BrTa(CO)_2(dppe)_2$ and $ClNb(CO)_2(dppe)_2$ showed a very small (0.1 μA) irreversible reduction wave near the solvent limit of CH_2Cl_2 at -1.8 V. Due to the proximity of the peak potentials to the dichloromethane solvent limit, these processes were not studied.

Chemical Oxidation of $ClNb(CO)_2(dppe)_2$. Several attempts to isolate the 17-electron species (ie $ClNb(CO)_2(dppe)_2^+$) via chemical oxidations were unsuccessful. Oxidation of $ClNb(CO)_2(dppe)_2$ with $[(Ph)_3C][PF_6]$ in CH_2Cl_2 at -70 °C resulted in the disappearance of the starting material at 1834 and 1759 cm^{-1}, but the oxidized species was not present in the infrared spectrum of the resulting solution. Oxidation of $ClNb(CO)_2(dppe)_2$ by $[Cp_2Fe][PF_6]$ in CH_2Cl_2 at -45 °C for 3 h gave a solution that contained ca. equal amounts of the neutral species and the oxidized species $ClNb(CO)_2(dppe)_2^+$. Several attempts to isolate a solid sample of the oxidized product from solutions of this type were unsuccessful.

A final attempt to generate $ClNb(CO)_2(dppe)_2^+$ by reacting $ClNb(CO)_2(dppe)_2$ with $AgPF_6$ in CH_2Cl_2 at -60 °C gave a black suspension that was filtered; an infrared spectrum of the resulting CH_2Cl_2 solution showed carbonyl peaks at 2029, 2017, 1960, and 1890 cm^{-1}. The product, most likely a silver complex, was not isolated. This reaction was not pursued further. No attempts to chemically oxidize $ITa(CO)_2(dppe)_2$, $INb(CO)_2(dppe)_2$, and $BrNb(CO)_2(dppe)_2$ were made.

Electrochemical Studies of $INb(CO)_2(dppe)_2$ in 0.1 M $TBA^+PF_6^-/CH_3CN$. The reduction chemistry of the $XM(CO)_2(dppe)_2$ complexes was studied in acetonitrile (solvent limits +2.0 V to −2.5 V). The cyclic voltammogram[17] of $INb(CO)_2(dppe)_2$ in 0.1 M $TBA^+PF_6^-/CH_3CN$ exhibits an irreversible two-electron reduction at $E_c = -1745$ mV with a coupled irreversible oxidation process at $E_a = -1381$ mV.

A series of infrared spectroelectrochemical experiments with $INb(CO)_2(dppe)_2$ in 0.1 M $TBA^+PF_6^-/CH_3CN$ were performed.[17] Figure 6 shows the reduction of $INb(CO)_2(dppe)_2$ at $E_{app} = -1800$ mV. The starting material with IR peaks at 1863 and 1790 cm^{-1} is converted to the anion, $Nb(CO)_2(dppe)_2^-$, (peaks at 1726 and 1667 cm^{-1}). When the complex is allowed to stand or after oxidation, the carbonyl peaks due to the anion disappeared to give a strong carbonyl peak at 1757 cm^{-1} that corresponds to $HNb(CO)_2(dppe)_2$. Reduction of the hydride (Figure 6a) at $E_{app} = -1800$ mV cleanly regenerates the anion. Again allowing the anion to stand regenerates hydride peaks at

(16) The two small peaks at 1840, and 1764 cm^{-1} correspond to an impurity of $ITa(CO)_2(dppe)_2$ that slowly formed during the course of the experiment (2 h).

(17) See supplementary material.

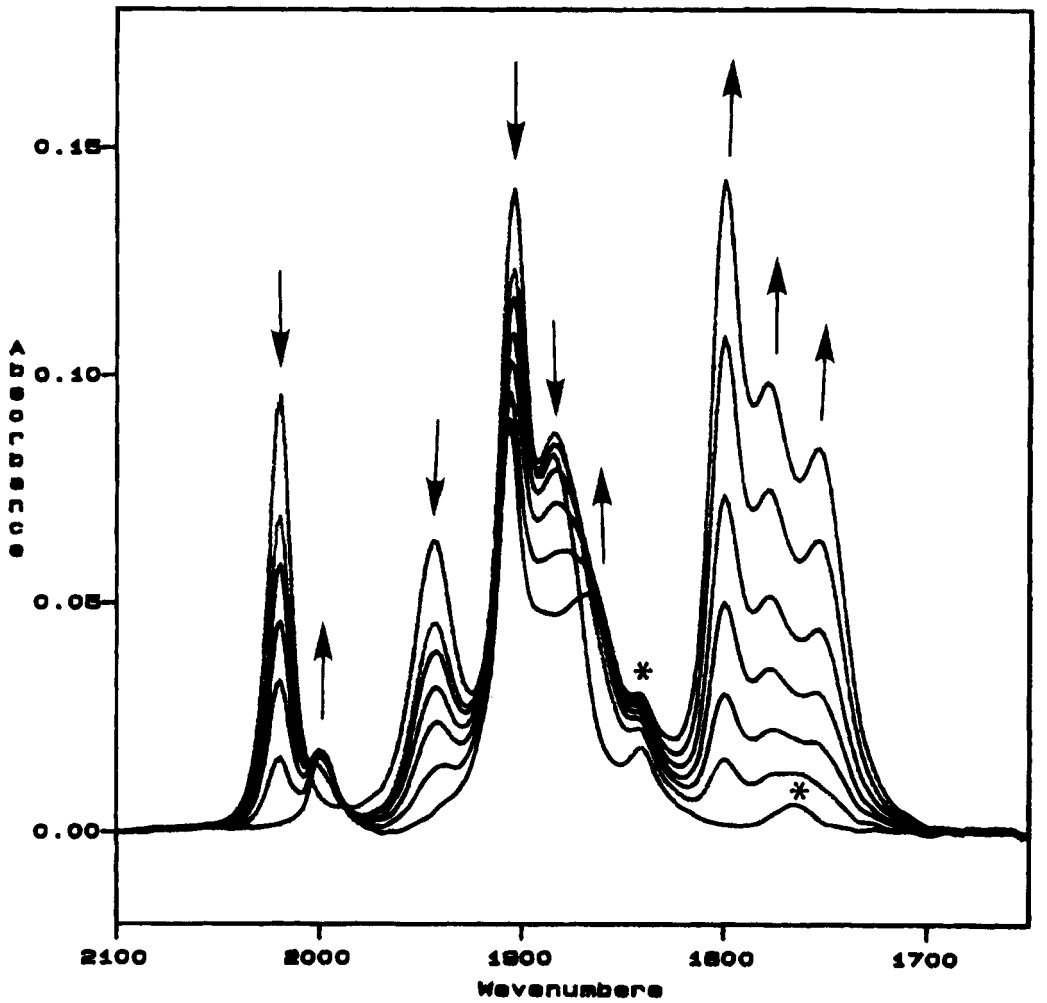

Figure 2. Infrared spectroelectrochemical reduction of $ITa(CO)_4(dppe)$ in 0.1 M $TBA^+PF_6^-$/THF at $E_{app} = -2000$ mV. Starred peaks are $ITa(CO)_2(dppe)_2$.

1757 cm^{-1}. Oxidation of hydride regenerates $INb(CO)_2(dppe)_2$ peaks 1863 and 1790 cm^{-1} along with a small amount of $HNb(CO)_2(dppe)_2^+$ with a peak at 1905 cm^{-1}. Analogous electrochemical behavior was observed in $TBA^+BF_4^-$/DME solutions. Reduction of $INb(CO)_2(dppe)_2$ at $E_{app} = -2100$ mV results in the generation of $Nb(CO)_2(dppe)_2^-$. Oxidation of the anion at $E_{app} = +500$ mV results in clean conversion to $HNb(CO)_2(dppe)$ $\nu(CO)$ at 1775 cm^{-1}.

Synthesis of $HM(CO)_2(dppe)_2$, (M = Nb, Ta). The assignment of the band at 1757 cm^{-1} as due to hydrido species in the spectroelectrochemical experiments was confirmed through the synthesis of the niobium and tantalum species. We have synthesized $HNb(CO)_2(dppe)_2$ and $HTa(CO)_2(dppe)_2$ by a new route with a higher yield than previously reported by Rehder *et al.*[14,18] Reduction of $ITa(CO)_2(dppe)_2$ with 40% Na(Hg) generated $[Na][Ta(CO)_2(dppe)_2]$; further treatment of this salt with excess EtOH gives $HTa(CO)_2(dppe)_2$ in 55% yield. $HNb(CO)_2(dppe)_2$ was synthesized in the same manner with an 85% yield. Both products were characterized by IR, ^1H NMR, ^{31}P NMR and elemental analysis (Experimental Procedures).

Electrochemical Studies of $HM(CO)_2(dppe)_2$ in 0.1 M $TBA^+PF_6^-/CH_2Cl_2$, Where M = Nb and Ta. $HNb(CO)_2(dppe)_2$ in 0.1 M $TBA^+PF_6^-/CH_2Cl_2$ exhibits cyclic voltammograms similar to the halide analogs. Several electrochemical processes are observed: a one-electron reversible reduction process at $E^{\circ\prime} = -272$ mV ($i_{p,c}/i_{p,a} = 1.0$), multielectron irreversible oxidation processes at $E_a = +732$ mV and $E_a = +1041$ mV, and a cathodic process at $E_c = +509$ mV coupled to the oxidation. The irreversible oxidations at potentials more positive than the reversible process were not investigated. Chronocoulometric data for the reversible wave at $E^{\circ\prime} = -272$ mV gives a value of $n = 1$ electron based on $D = 2.69 \times 10^{-6}$ cm^2/s.[19] This electrochemical process generated the 17-electron hydride radical (eq 2).

$$HNb(CO)_2(dppe)_2 \rightleftharpoons HNb(CO)_2(dppe)_2^+ + e^- \quad (2)$$

The tantalum analog shows similar behavior with a reversible one-electron process at $E^{\circ\prime} = -264$ mV ($i_{p,c}/i_{p,a} = 1.0$) and multielectron irreversible processes at $E_a = +796$ mV and $E_a = +1027$ mV. The diffusion coefficient in this case for $n = 1$ electron is 2.87 x 10^{-6} cm^2/s.

The infrared spectroelectrochemistry of $HNb(CO)_2(dppe)_2$ at $E_{app} = +400$ mV (Figure 7) shows the isosbestic conversion of $HNb(CO)_2(dppe)_2$ (peaks at 1765 cm^{-1}) to the radical hydride species, $HNb(CO)_2(dppe)_2^+$, (peaks at 1900 cm^{-1}).[20] The cation radical can be quantitatively reduced at $E_{app} = -500$ mV to

(18) Fornalcyzk, F.; Sussmilch, F.; Priebsch, W.; Rehder, D. *J. Organomet. Chem.* **1992**, *426*, 159.

(19) During the course of the electrochemical experiments with $HMNb(CO)_2(dppe)_2$, a new reversible electrochemical process grew in at $E^{\circ\prime} = -7$ mV. This process corresponds to the oxidation of $ClNb(CO)_2(dppe)_2$. $HNb(CO)_2(dppe)_2$ slowly reacts with the CH_2Cl_2 solvent to generate $ClNb(CO)_2(dppe)_2$ in the bulk solution. Stirring $HNb(CO)_2(dppe)_2$ in CH_2Cl_2 for 4.5 h results in conversion of one-third of the $HNb(CO)_2(dppe)_2$ to $ClNb(CO)_2(dppe)_2$. Experiments with chloroform gave similar results.

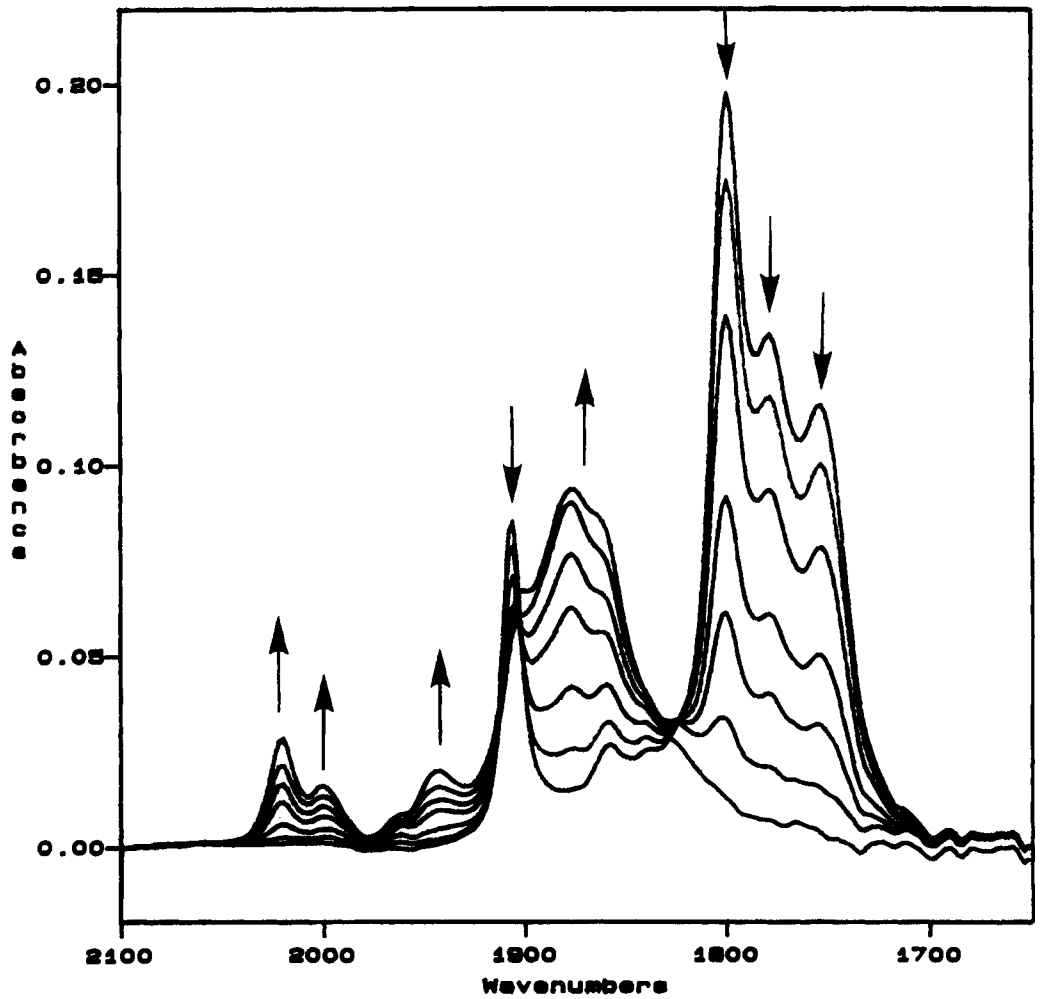

Figure 3. Infrared spectroelectrochemical oxidation of $Ta(CO)_4(dppe)^-$ in 0.1 M $TBA^+PF_6^-/THF$ at $E_{app} = -300$ mV.

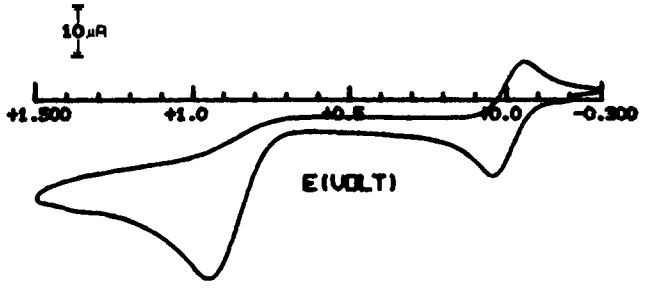

Figure 4. Cyclic voltammogram of $ClNb(CO)_2(dppe)_2$ in 0.1 M $TBA^+PF_6^-/CH_2Cl_2$ at a scan rate of 100 mV/s.

regenerate the neutral hydride species. Further oxidation of $HNb(CO)_2(dppe)_2$ at $E_{app} = +1000$ mV results in the appearance of both $HNb(CO)_2(dppe)_2^+$ and $ClNb(CO)_2(dppe)_2^+$.

$HTa(CO)_2(dppe)_2$ (peak at 1754 cm^{-1}) gives analogous spectroelectrochemical results with conversion to the cationic species (peak at 1877 cm^{-1}).

Electrochemical Studies of $HNb(CO)_2(dppe)_2$ in 0.15 M $TBA^+BF_4^-$/DME. $HNb(CO)_2(dppe)_2$ was studied in 0.15 M $TBA^+BF_4^-$/DME to eliminate the formation of the chloro species. Under these conditions, the cyclic voltammogram shows a reversible one-electron oxidation process at $E^{o\prime} = -59$ mV ($i_{pc}/i_{pa} = 0.87$) and a multielectron irreversible process at $E_a = +800$ mV. As in the CH_2Cl_2 case, the infrared spectroelectrochemistry at $E_{app} = +1000$ mV shows the smooth conversion of starting material (peak at 1775 cm^{-1}) to the cationic species (peak at 1898 cm^{-1}).

Chemical Oxidation of $HNb(CO)_2(dppe)_2$. As in the case of the $ClNb(CO)_2(dppe)_2^+$ radical cation, $HNb(CO)_2(dppe)_2^+$ was also stable on the electrochemical time scale. Chemical oxidation of $HNb(CO)_2(dppe)_2$ with 0.75 equiv of ferrocenium hexafluorophosphate in THF at room temperature resulted in a 50% conversion to the radical cation after 2 h, but attempts to isolate salts of $HNb(CO)_2(dppe)_2^+$ were unsuccessful.

(20) The other small carbonyl peaks in the spectrum correspond to neutral and oxidized bands of the analogous chloro species.

Table 1. Electrochemical Data for the Oxidation of $XM(CO)_2(dppe)_2$ Complexes in 0.1 M $TBA^+PF_6^-/CH_2Cl_2$

compound	$E^{o\prime}$ (V)[b]	10^6D (cm^2/s)[c]	$E_{p,a} - E_{p,c}$ (V)[d]	$i_{p,c}/i_{p,a}$
$ITa(CO)_2(dppe)_2$	+0.000	1.52	0.078	0.94
	+0.929[a]			
$HTa(CO)_2(dppe)_2$	−0.264	2.87	0.084	1.0
	+0.796[a]			
$INb(CO)_2(dppe)_2$	+0.110	4.29	0.097	0.96
	+0.999[a]			
$BrNb(CO)_2(dppe)_2$	+0.014	3.32	0.091	1.0
	+0.925[a]			
$ClNb(CO)_2(dppe)_2$	−0.007	2.05	0.100	0.84
	+0.960[a]			
$HNb(CO)_2(dppe)_2$	−0.272	2.69	0.088	1.0
	+0.732[a]			
$HNb(CO)_2(dppe)_2$[e]	−0.059	4.51	0.127	0.87
	+0.800[a]			

[a] Peak potential. [b] Potentials versus Ag/AgCl in 1.0 M KCl. [c] Determined by double-potential step chronocoulometry. [d] Scan rate = 100 mV/s. [e] $TBA^+BF_4^-$/DME.

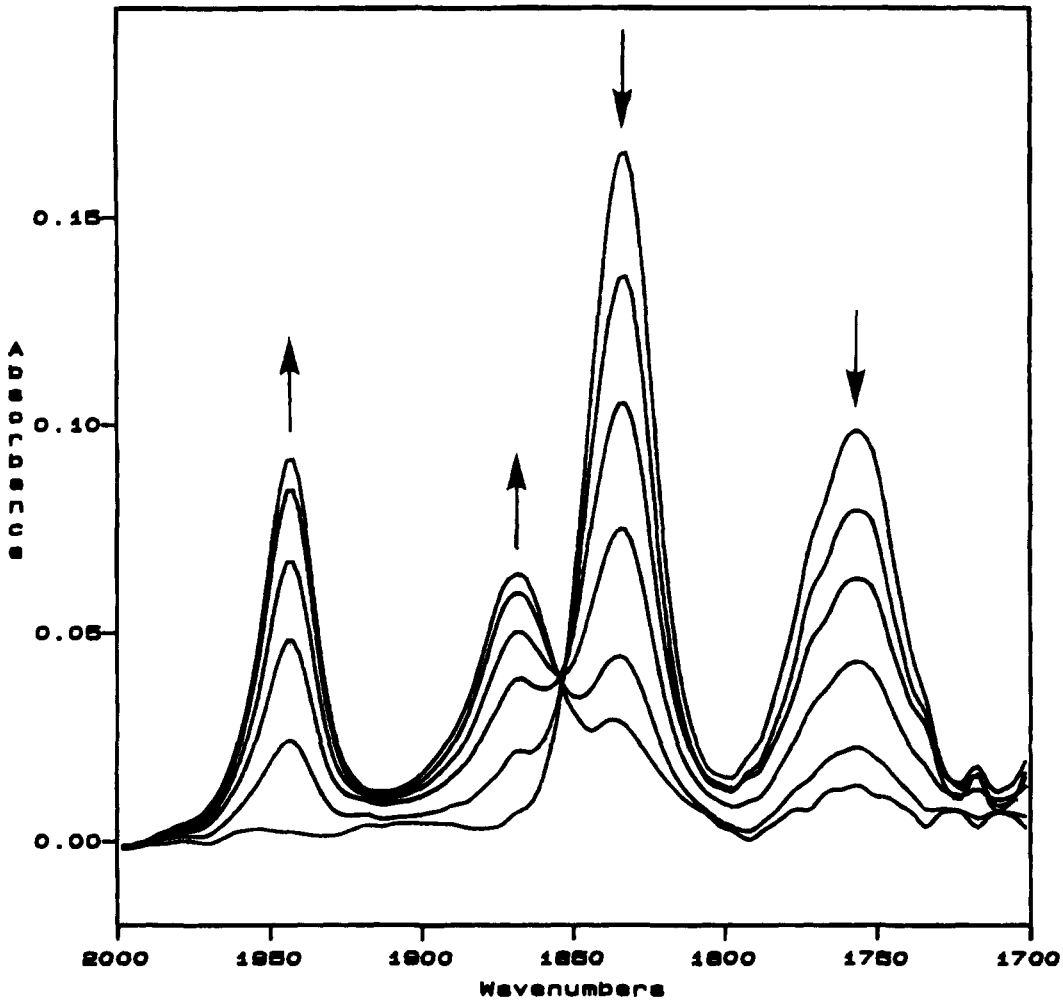

Figure 5. Infrared spectroelectrochemical oxidation of $ClNb(CO)_2(dppe)_2$ in 0.1 M $TBA^+PF_6^-/CH_2Cl_2$ at E_{app} = +400 mV.

Table 2. Infrared Spectroelectrochemical Data (cm^{-1}) for the Oxidation of $XM(CO)_2(dppe)_2$ in 0.1 M $TBA^+PF_6^-$ in CH_2Cl_2

compound	$XM(CO)_2(dppe)_2$	$XM(CO)_2(dppe)_2^+$
$ITa(CO)_2(dppe)_2$	1832, 1753	1928, 1849
$HTa(CO)_2(dppe)_2$	1754	1898
$INb(CO)_2(dppe)_2$	1838, 1759	1942, 1869
$BrNb(CO)_2(dppe)_2$	1838, 1757	1944, 1869
$ClNb(CO)_2(dppe)_2$	1834, 1759	1944, 1869
$HNb(CO)_2(dppe)_2$	1765	1900
$HNb(CO)_2(dppe)_2$[a]	1775	1877

[a] $TBA^+BF_4^-$/DME.

Table 3. Electrochemical Data for the Reduction of $XTa(CO)_4(dppe)_2$ and $INb(CO)_2(dppe)_2$ at a Scan Rate of 100 mV/s

compound	$E_{cathodic}$ (V)	coupled E_{anodic} (V)
$BrTa(CO)_4(dppe)_2$[a]	−1.332	−0.742; −0.121
$ITa(CO)_4(dppe)_2$[a]	−1.731	−0.708; −0.021
$ITa(CO)_4(dppe)_2$[b]	−1.541	−0.530; +0.100
$INb(CO)_2(dppe)_2$[c]	−1.745	−1.381
$INb(CO)_2(dppe)_2$[d]	−2.206	−1.240

[a] 0.1 M $TBA^+PF_6^-/CH_2Cl_2$. [b] 0.1 M $TBA^+PF_6^-$/THF. [c] 0.1 M $TBA^+PF_6^-/CH_3CN$. [d] 0.1 M $TBA^+BF_4^-$/DME.

EPR Data for $ClNb(CO)_2(dppe)_2^+$ and $HNb(CO)_2(dppe)_2^+$. Although we were unable to isolate solid samples containing $ClNb(CO)_2(dppe)_2^+$ and $HNb(CO)_2(dppe)_2^+$, we electrochemically generated the radical cations in a thin layer bulk electrolysis cell, transferred the solutions into an EPR tube at −78 °C, and obtained the EPR spectrum of $ClNb(CO)_2(dppe)_2^+$ at 77 K (Figure 8a). The EPR spectrum showed the 10-line pattern expected for the unpaired electron coupling to the niobium nucleus (^{93}Nb (I = 9/2)), at g = 2.04 relative to the DPPH standard. The Nb coupling is 115 G. No resolved phosphorus coupling is evident in the spectrum.

Table 4. Infrared Spectroelectrochemical Data (cm^{-1}) for the Reduction of $XTa(CO)_4(dppe)_2$ and $INb(CO)_2(dppe)_2$ and the Subsequent Oxidations of the Anions

compound	ν(CO) stretch	$Ta(CO)_4(dppe)^-$	oxidized products
$ITa(CO)_4(dppe)_2$[a]	2020, 1944, 1904	1906, 1880, 1778	$HTa(CO)_4(dppe)$
	1884 cm^{-1}	1753	1998, 1867 + starting material

compound	ν(CO) stretch	$Nb(CO)_2(dppe)_2^-$	oxidized products
$INb(CO)_2(dppe)_2$[b]	1863, 1790	1726, 1667	$HNb(CO)_2(dppe)_2$ 1757
$INb(CO)_2(dppe)_2$[c]	1845, 1770	1730, 1660	$HNb(CO)_2(dppe)_2$ 1763

[a] 0.1 M $TBA^+PF_6^-$/THF. [b] 0.1 M $TBA^+PF_6^-/CH_3CN$. [c] 0.1 M $TBA^+BF_4^-$/DME.

The EPR spectrum of $HNb(CO)_2(dppe)_2^+$ in 0.1 M $TBA^+PF_6^-/CH_2Cl_2$ at 77 K was also obtained and is shown in Figure 8b. The spectrum of the cation hydride radical showed a 10-line pattern at g = 2.05, with niobium hyperfine coupling of 113 G. The EPR spectrum of $HNb(CO)_2(dppe)_2^+$ showed some additional super hyperfine splitting due to either the hydride or the phosphorus ligands. Further analysis of this EPR spec-

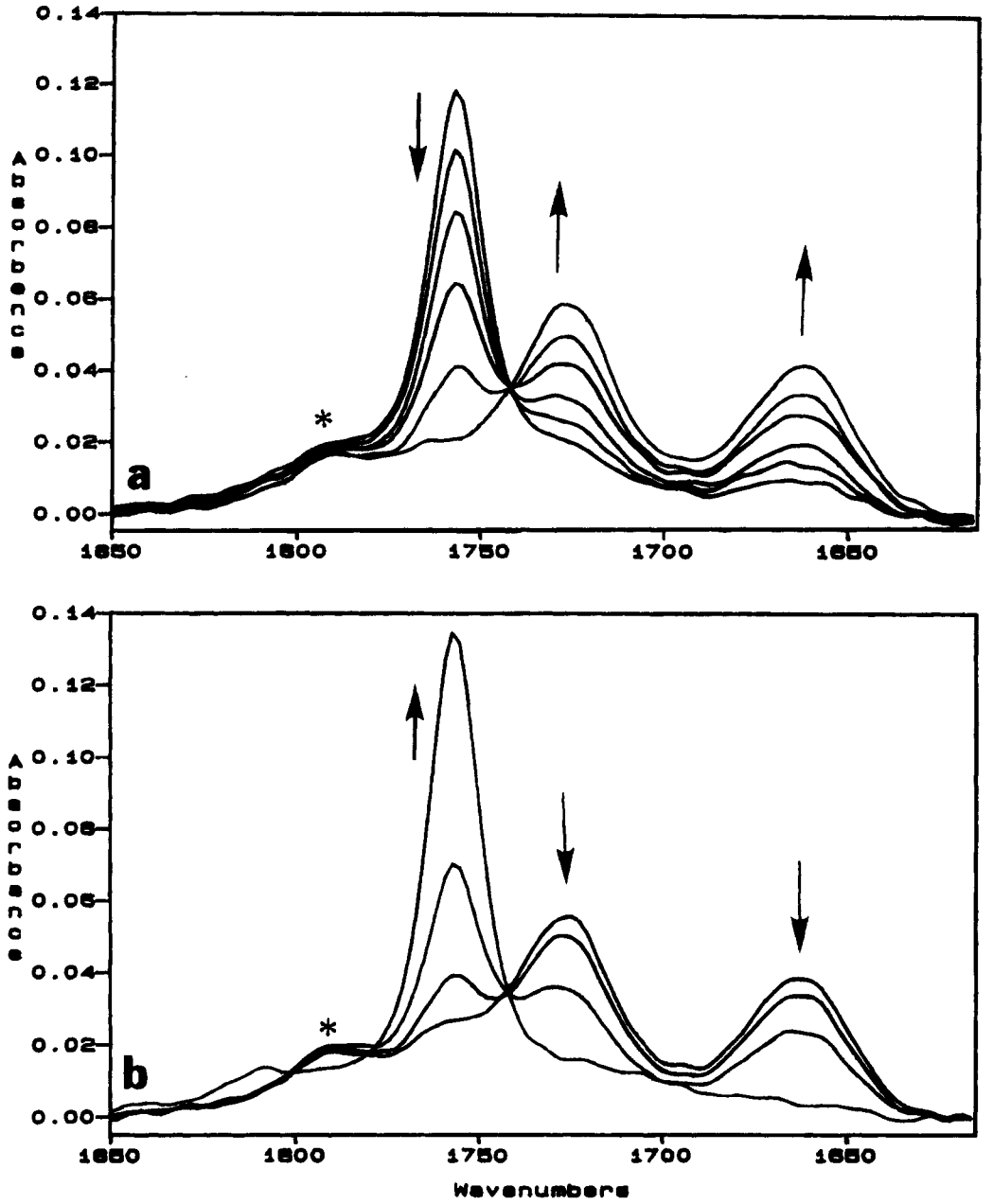

Figure 6. (a) Infrared spectroelectrochemical reduction of $HNb(CO)_2(dppe)_2$ in 0.1 M $TBA^+PF_6^-/CH_3CN$ at $E_{app} = -1800$ mV. (b) regeneration of the hydride species upon standing in the spectroelectrochemical cell. Starred peak is $INb(CO)_2(dppe)_2$.

tra will be needed to unravel the origin of these additional splittings.

Discussion

We have studied the electrochemistry of $XTa(CO)_4(dppe)$ (X = I, Br) and $XM(CO)_2(dppe)_2$, where X = I, Br, and Cl and M = Nb and Ta. The substitution of two additional carbonyls with the electron-rich dppe ligand produces complexes that differ considerably in their redox behavior. The $XM(CO)_2(dppe)_2$ complexes are reduced with more difficulty but are more easily oxidized than the $XTa(CO)_4(dppe)$ complexes. For example, the reduction potential of $ITa(CO)_4(dppe)$ is 200 mV more negative than that observed for $INb(CO)_2(dppe)_2$, but the oxidation potentials are ca. 850 mV more positive. The electrochemical reduction of both the tetracarbonyl and the dicarbonyl complexes result in the production of anions (ie. $Ta(CO)_4(dppe)^-$ and $Nb(CO)_2(dppe)_2^-$) that are rapidly protonated by adventitious water, particularly in the case of the dicarbonyl complexes, to give the corresponding hydrides ($HTa(CO)_4(dppe)$ and $HNb(CO)_2(dppe)_2$). The oxidation chemistry of the seven-coordinate (+I) metal center in these complexes is more variable. Electrochemical oxidation of the tetra carbonyl complexes results in a multielectron oxidation to products that do not contain carbon monoxide; the bis carbonyl complexes form, on oxidation, stable 17-electron radical species, $XM(CO)_2(dppe)_2^+$ (Table 1).

The reductions of $ITa(CO)_4(dppe)$ in dichloromethane or tetrahydrofuran and $INb(CO)_2(dppe)_2$ in acetonitrile were particularly amenable for study. $ITa(CO)_4(dppe)$ exhibits a clean two-electron reduction that generates $Ta(CO)_4(dppe)^-$. The infrared carbonyl stretching frequencies of $Ta(CO)_4(dppe)^-$ observed in the spectroelectrochemical cell were consistent with values reported by Wreford and co-workers for similar compounds.[18] In each solvent, a small of amount of $HTa(CO)_4(dppe)$ was generated upon reduction due to trace amounts of water in solution. Oxidation of the anion in dichloromethane occurs at −708 mV, while oxidation of the hydride occurs at

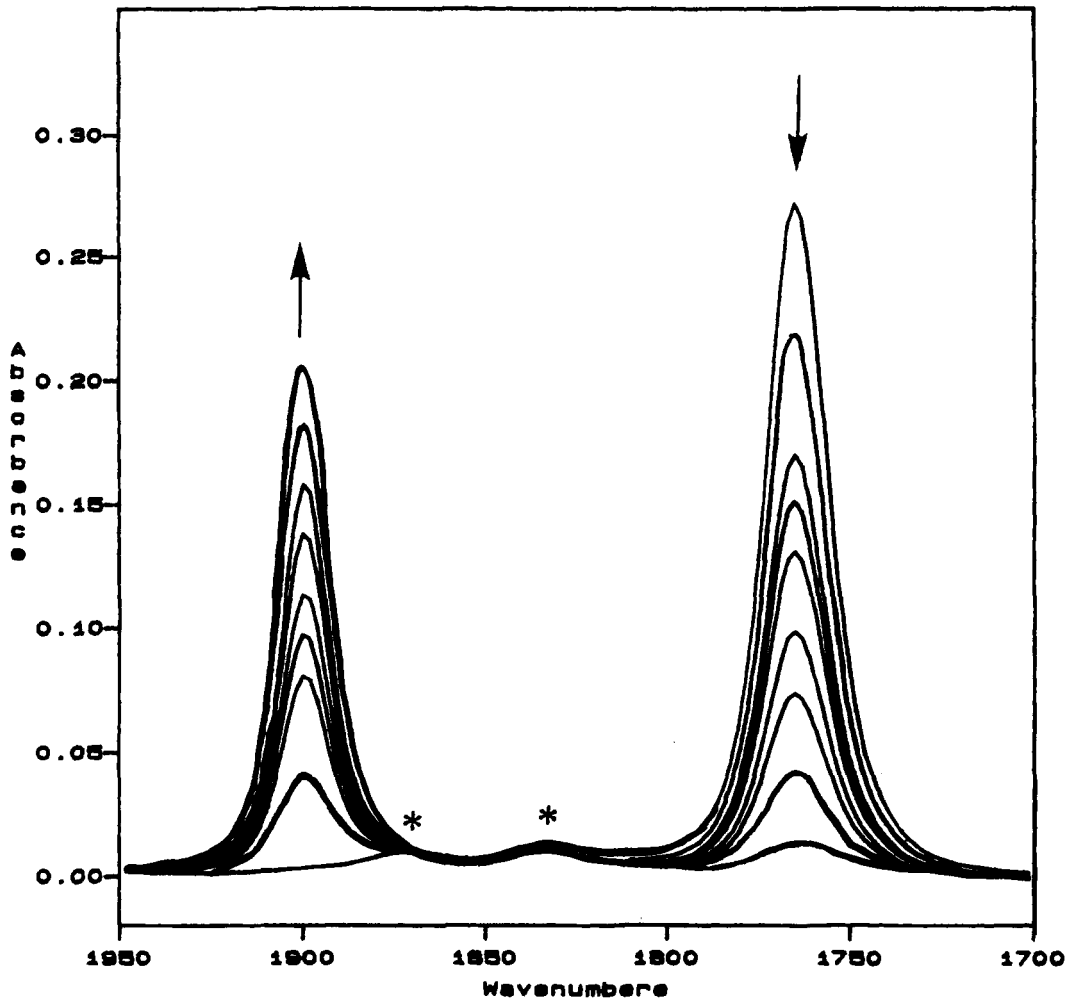

Figure 7. Infrared spectroelectrochemical oxidation of $HNb(CO)_2(dppe)_2$ in 0.1 M $TBA^+PF_6^-/CH_2Cl_2$ at E_{app} = +400 mV. Starred peaks are neutral and oxidized $ClNb(CO)_2(dppe)_2$.

−21 mV. In THF, these processes are shifted to −530 and +100 mV, respectively.

The facile reduction of $ITa(CO)_4(dppe)$ to $Ta(CO)_4(dppe)^-$ afforded an opportunity to attempt the generation of the recently reported 17-electron radical $Ta(CO)_4(dppe)^2$ via oxidation of $Ta(CO)_4(dppe)^-$. In 0.1 M $TBA^+PF_6^-/CH_2Cl_2$, the spectroelectrochemical oxidation at E_{app} = −300 mV generates a broad peak[21] at 1881 cm^{-1} and two small carbonyl peaks corresponding to the starting material, $ITa(CO)_4(dppe)$. We assign the 1881 cm^{-1} peak to a mixture of $HTa(CO)_4(dppe)$ and $ITa(CO)_4(dppe)$. We attribute the formation of the hydride to a reaction of an unobserved, oxidized species with the trace amounts of water remaining in the carefully dried solvent and supporting electrolyte mixture. The final spectrum of this oxidation sequence shows only carbonyl peaks corresponding to the starting material, $ITa(CO)_4(dppe)$. A plausible explanation for the regeneration of starting material from $HTa(CO)_4(dppe)$ is through reaction[22] of I_2 with $HTa(CO)_4(dppe)$, followed by a reaction of the resulting HI with $HTa(CO)_4(dppe)$ to evolve hydrogen gas and $ITa(CO)_4(dppe)$. Alternatively, replacement of hydride by iodide could occur in the oxidized form of $HTa(CO)_4(dppe)$ (vide infra).

Oxidation of $Ta(CO)_4(dppe)^-$ in THF gives results similar to those in CH_2Cl_2; however, a greater amount of the hydride was generated. If a large excess of H_2O relative to the iodide produced on reduction is deliberately added to the THF solutions, reduction of $ITa(CO)_4(dppe)$ generates $Ta(CO)_4(dppe)^-$ and $HTa(CO)_4(dppe)$ as before, but subsequent oxidation of the anion results in clean conversion to $HTa(CO)_4(dppe)$. Although it is likely that the reactive, oxidized species in all of the oxidation reactions of $Ta(CO)_4(dppe)^-$ is $Ta(CO)_4(dppe)$, there is no direct spectrocopic evidence to support this idea.

The results with $Ta(CO)_4(dppe)^-$ suggested that a similiar investigation of the more electron rich and sterically congested $INb(CO)_2(dppe)_2$ system might yield the direct observation of the $Nb(CO)_2(dppe)_2$ radical. The reduction of $INb(CO)_2(dppe)_2$ in acetonitrile occurs at very negative potentials, but a two-electron reduction product, $Nb(CO)_2(dppe)_2^-$, is obtained as in the case of the Ta complex. The carbonyl stretching frequencies for the Nb anion are in good agreement with the dmpe analog reported by Lippard and co-workers.[1] As in the Ta case, the anion slowly converts on standing or oxidation to $HNb(CO)_2(dppe)_2$ with ν(CO) at 1757 cm^{-1}. Again we conclude that the small amounts of water in the carefully dried solvents/supporting electrolyte causes protonation of the anion to produce the hydride. We view as much less likely the deprotonation of acetonitrile to form CH_2CN^-, although precedence for an analogous reaction is observed in group VI anion chemistry.[23] As in the case of the oxidation of $HTa(CO)_4(dppe)$ in the presence of iodide, oxidation of $HNb(CO)_2(dppe)_2$ produces $INb(CO)_2(dppe)_2$ and no direct evidence for a putative $Nb(CO)_2(dppe)_2$ radical species. Similar behavior is observed in the

(21) These carbonyl stretching frequencies are in excellent agreement with ν(CO) values reported by Wreford and co-workers for analogous compounds.[24]

(22) The I_2 may result from the oxidation of I^-.

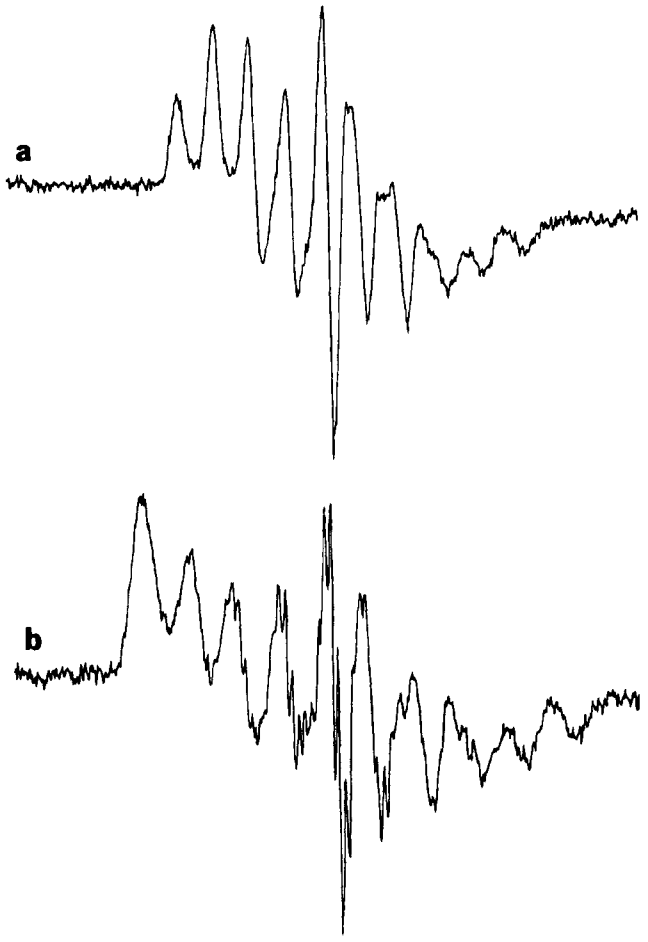

Figure 8. (a) EPR spectrum of $ClNb(CO)_2(dppe)_2^+$ in 0.1 M $TBA^+PF_6^-$ at 77 K. (b) EPR spectrum of $HNb(CO)_2(dppe)_2^+$ in 0.1 M $TBA^+PF_6^-$ at 77 K.

group VI analogs of these complexes where the hydride is converted to the iodo species upon standing in solution.[24]

All the interconversions between the anion, hydride, and iodide species reported above for these group V species are analogous to behavior observed in group VI chemistry. For example, oxidation of $Mo(CO)_2(dmpe)_2$ with $[NO][PF_6]$ yields, as the only product the Mo(II) hydride, $HMo(CO)_2(dmpe)_2^+$.[27] Moreover, our results are consistent with those of Wreford and co-workers who suggested that the presence of the hydride in the reduction of $ClTa(CO)_2(dmpe)_2$ resulted from trace amounts of water in the system.[24] The apparent stability and facile oxidation chemistry we observed for electrochemically generated $HNb(CO)_2(dppe)_2$ and $HTa(CO)_2(dppe)_2$ prompted us to improve the syntheses of these hydride species. These synthetic improvements have allowed comparisons of the electrochemical oxidation chemistry of the seven coordinate, M(I) hydride species with the halides.

Oxidation studies of $XTa(CO)_4(dppe)$ and $XM(CO)_2(dppe)_2$, where X = I, Br, Cl, and H and M = Nb and Ta, show that the substitution of two carbonyl ligands for a dppe ligand greatly enhances the stability of the M(II) oxidation state. The standard potential for the oxidation of $ITa(CO)_4(dppe)$ is 850 mV more positive than that of $ITa(CO)_2(dppe)_2$. The stability of the oxidized form in each case also differs dramatically. The tetracarbonyl complexes exhibit an irreversible process that results exclusively in non-carbonyl containing products while the dicarbonyl complexes oxidize in one-electron reversible processes that generate stable, seven-coordinate 17-electron species (ie $ITa(CO)_2(dppe)_2^+$) (see Table 1). In most respects, the electrochemical oxidation experiments with the hydride complexes ($HM(CO)_2(dppe)_2$) were comparable to those of the halides; oxidation resulted in the generation of the 17-electron hydride radical. A complication arose in the electrochemistry of $HNb(CO)_2(dppe)_2$ performed in CH_2Cl_2. Chloride was abstracted by the hydride species from the solvent to generate $ClNb(CO)_2(dppe)_2$. Independent solution studies in dichloromethane and chloroform confirmed these halide abstraction reactions. The observed potentials followed the trend I > Br > Cl > H and Nb > Ta, with the iodo analog and niobium analogs most difficult to oxidize compared to the hydrido and tantalum analogs. The dppe compounds studied here are comparable in most respects to the dmpe analogs studied by Wreford and co-workers.[24]

Several attempts to synthesize and isolate salts of the 17-electron oxidation products via chemical oxidation (ferricinium, trityl cation, Ag^+) were unsuccessful. Similar attempts to isolate the hydride containing radical species via chemical oxidation were also unsuccessful. In all cases investigated the radicals are stable on the electrochemical time scale, and the radicals are present in chemically oxidized solutions but removal of the solvent causes loss of carbon monoxide to generate non-carbonyl-containing products.

Even though we were unable to isolate the seven coordinate radical species, we were able to successfully characterize them in solution. IR spectroscopy showed that in each case the ν-(CO) stretch(s) observed for the unoxidized, seven coordinate parent shifts to higher energy ($\sim$100 cm^{-1}) and the pattern remains unchanged (a single band for the hydride complexes with presumably nearly trans CO's and two bands for the halide complexes). The similar relative intensities of the neutral and cationic halide complex absorption peaks suggests that no major changes in geometry occur upon oxidation. This behavior contrasts the chemistry observed for the analogous group VI compounds in which cis−trans isomerization results on oxidation.[25-30] The change in bond angle between the two cis carbonyls upon oxidation is determined by measuring the relative intensities of the CO peaks.[31] These calculations indicate a 2° change upon oxidation for $ClNb(CO)_2(dppe)_2$, 5° for $BrNb(CO)_2(dppe)_2$, and 8° for $INb(CO)_2(dppe)_2$. The increase in the angle change is expected for the increasing size of the halide.

We were also able to characterize the seven coordinate radical species by EPR spectroscopy. Oxidation of $ClNb(CO)_2(dppe)_2$ or $HNb(CO)_2(dppe)_2$ in a thin-layer, bulk electrolysis cell generated solutions of $ClNb(CO)_2(dppe)_2^+$ or $HNb(CO)_2(dppe)_2^+$, respectively that were stable enough to obtain EPR spectra. For the $ClNb(CO)_2(dppe)_2^+$ complex, the expected 10-line pattern was observed in the EPR spectrum, consistent with localization of the electron on the niobium ($I = {}^9/_2$) nucleus. The hyperfine coupling constant for the niobium coupling was 115 G. As far as we are aware, this is the first niobium(II)

(23) Connelly, N. G.; Davis, R. L. *Organomet. Chem.* **1976**, *120*, C16.
(24) Datta, S.; McNeese, T. J.; Wreford, S. S. *Inorg. Chem.* **1977**, *16*, 2661.
(25) Datta, S.; Dezube, B.; Kouba, J. K.; Wreford, S. S. *J. Am. Chem. Soc.* **1978** *100*, 404.
(26) Holden, L. K.; Mawby, A. H.; Smith, D. C.; Whyman, R. *J. Organomet. Chem.* **1973**, *55*, 343.
(27) Snow, M. R.; Wimmer, F. L. *Aust. J. Chem.* **1976**, *29*, 2349.
(28) Conner, J. A.; Riley, P. I.; Rix, C. J. *J. Chem. Soc., Dalton. Trans.* **1977**, 1317.
(29) Blagg, A.; Carr, S. W.; Cooper, G. R.; Dobson, I. D.; Gill, J. B.; Goodall, D. C.; Shaw, B. L.; Taylor, N.; Boddington, T. *J. Chem. Soc., Dalton. Trans.* **1985**, 1213.
(30) Bond, A. M.; Colton, R.; McGregor, K. *Organometallics* **1990**, *9*, 1227.
(31) Cotton, F. A.; Wilkinson, G. *Advanced Inorganic Chemistry*; John Wiley and Sons: New York, 1988; pp 1035−1037.

carbonyl radical species reported in the literature. Moreover, only one Nb(II) complex was found, Cp_2Nb.[32] Most of the EPR data reported for Nb are Nb(IV) species.[33-37] The coupling constants we observe are in good agreement with these reported niobium(IV) radicals.

The EPR spectrum of the $HNb(CO)_2(dppe)_2^+$ exhibits a 10-line pattern similar to the chloride complex, with a niobium coupling constant of 113 G. In this case, five to eight line superhyperfine splitting pattern is observed with a coupling constant of ~17 G. The interpretation of this coupling constant is not possible, because it lies between the typical Nb−P coupling constant of 26 G and the Nb−H coupling constant of 11 G. Simulation of the coupling pattern with four equivalent phosphorus nuclei gives a spectrum similar to the experimental spectrum. Simulation with two inequivalent sets of two phosphorus atoms also produced spectra that somewhat resembled the observed spectrum. In either case, the doublet pattern observed for each peak was not simulated by the phosphorus coupling. We tentatively suggest this additional splitting might be due to coupling to the hydride ligand. Data of substantially higher quality will be needed to solidify these assignments.

Conclusions

We have performed electrochemical studies with the substituted carbonyl complexes $XTa(CO)_4(dppe)_2$ and $XM(CO)_2(dppe)_2$. Electrochemical results showed enhanced stability of the one electron oxidized form of the dicarbonyl compounds compared to the tetracarbonyl compounds. The electron-donating ability of the dppe ligand greatly enhances the stability of the bis carbonyl compounds. Electrochemical results showed the high relative stability of the (+I) and (−I) oxidation states for niobium and tantalum, compared to the seemingly unaccessible zerovalent state.

Electrochemical oxidation of $ClNb(CO)_2(dppe)_2$ and $HNb(CO)_2(dppe)_2$ in the thin-layer bulk electrolysis cell resulted in the detection of the first 17-electron radical species of group V substituted carbonyl complexes.

Acknowledgment. This research is supported by the National Science Foundation under Grants No. CHE-9307837 (K.R.M.) and No. CHE-9113242 (J.E.E.). C.A.B. would like to thank the University of Minnesota and Air Products Co. for a Pre-Doctoral Fellowship.

Supplementary Material Available: Figures showing the IR oxidation of $Ta(CO)_4(dppe)^-$, cyclic voltammogram of $INb(CO)_2(dppe)_2$, and the IR reduction of $INb(CO)_2(dppe)_2$ (3 pages). Ordering information is given on any current masthead page.

IC941056V

(32) Lemenovskii, D. A.; Fedin, V. P. *J. Organomet. Chem.* **1977**, *132*, C11.
(33) Elson, I. E.; Kochi, J. K.; Klabunde, U.; Manzer, L. E.; Parshall, G. W.; Tebbe, F. N. *J. Am. Chem. Soc.* **1974**, *96*, 7374.
(34) Elson, I. H.; Kochi, J. K. *J. Am. Chem. Soc.* **1975**, *97*, 1262.
(35) Al-Mowali, A. H.; Kuder, W. A. A. *J. Organomet. Chem.* **1980**, *194*, 61.
(36) Hitchcock, P. B.; Lappert, M. F.; Milne, C. R. C. *J. Chem. Soc., Dalton. Trans.* **1981**, 180.
(37) Luetkens, Jr., M. L.; Elcesser, W. L.; Huffman, J. C.; Sattelberger, A. P. *J. Am. Chem. Soc.* **1984**, *23*, 1718.